ELECTROMIGRATION DEGRADATION MODEL OF METAL OXIDE VARISTOR STRUCTURES

A.V. IVANCHENKO,[1] A.S. TONKOSHKUR[2]

[1]**Ukrainian State Chemical-Technology University**
(8, Prosp. Gagarina, Dnepropetrovsk 49005, Ukraine; e-mail: ivanchenkoav@ukr.net)

[2]**Oles Honchar National University of Dnipropetrovsk**
(72, Prosp. Gagarina, Dniepropetrovsk 49010, Ukraine; e-mail: tonkoshkuras@mail.ru)

PACS 73.40.Ty; 84.32.Ff

Ion migration in zinc-oxide semiconductor crystallites at long periods of the current flow has been simulated, and its influence on the current-voltage characteristics (CVCs) of varistor structures has been analyzed. The conditions and the parameters suitable for monitoring the process of varistor-structure irreversible degradation have been determined.

A component of the intergrain potential barrier generated by the space charge region in a crystallite, which turns out reverse-biased at the degradation current flow, was found to be the most prone to changes (the accumulation of near-surface donors, and a reduction of the barrier height and thickness). During the degradation, the varistor section in the direct (with respect to the degradation current) CVC branches becomes more shifted toward lower voltages, whereas the leakage current is more growing in the weakly linear section of the reverse CVC branch.

An agreement was obtained between the change tendencies predicted by a developed model for main varistor parameters (a reduction of the classification voltage, a reduction of the nonlinearity factor, and an increase of the leakage current) and the available experimental data. A possibility to estimate the diffusion coefficient of charged donors and to use this parameter to monitor the functionability of devices based on zinc oxide varistor structures with tunnel current-voltage characteristics has been demonstrated.

1. Introduction

The problem of degradation of varistors and other electronic elements developed on the basis of nonlinear zinc oxide ceramics in the course of their exploitation arose practically simultaneously with the beginning of their wide application. Hitherto, this problem remains one of the least studied ones, although being a subject of a considerable number of researches [1–7].

Recently, the following reasons giving rise to a drift of zinc-oxide ceramics electric parameters have been established: polarization processes associated with the motion of free electrons and their capture by energy traps [7–9], adsorption-desorption of oxygen in the course of heating [10, 11], and migration of ions in an electric field (as a rule, also at elevated temperatures) [2,3,12,13]. The first two mechanisms of degradation are classed as invertible ones, and they are most studied. In particular, quantitative theoretical models are developed for them [14, 15], as well as technological methods for restoring the nonlinear current-voltage characteristic (CVC) of varistor structures (heating up the varistors with short-circuited electrodes and holding them in an oxygen-containing environment) [11].

The third mechanism is irreversible. According to the modern conceptions, the degradation, which is governed by this mechanism, arises as a result of the field-stimulated diffusion of interstitial zinc [2, 16] or some other ions of technological additives, which can occupy interstitial sites–in particular, these are Co ions in the near-boundary depleted layer of ZnO crystallite,–which is accompanied by the chemical interaction with defects of the crystallite–boundary type. Just this process gives rise to a reduction of the barrier height and an increase of the leakage current. The origin of interstitial zinc is associated with the nonstoichiometric nature of ZnO. The latter, when being heated even in an oxidizing environment, can form excess zinc donors at interstitial sites, which become "frozen", when being cooled down to room temperature [2].

The degradation associated with the ionic migration is less studied, which is evidently related to mathemat-

ical difficulties arising when considering a deviation of the shape of intergrain potential barriers in the varistor structure from the Schottky one. The available models describing the evolution of this degradation either have an empirical character [3, 17] or are based on an approximate solution obtained for the heat conductivity equation in the absence of an electric field [16]. Therefore, despite that a definite technological progress was achieved – in particular, a certain decrease in the rate of irreversible degradation was obtained by varying metal oxide additives to the ceramic content (e.g., an insertion of boron oxide [18, 19]), – the absence of a consistent theoretical model, which would describe electron-molecular processes in ceramics, does not allow one to understand this kind of degradation in the examined inhomogeneous structure and to predict a distortion of CVCs for varistor products on its basis.

In this work, we report the results of simulation of the ion migration in zinc oxide semiconductor crystallites in an electric field and, using the terminology of work [20], its influence on CVCs of varistor structures with the tunnel mechanism of electrical conductivity. We also determined the conditions and the electric parameters, which are suitable for monitoring the process of varistor structure degradation. The following main characteristics were analyzed: the distribution of a charged donor impurity, the shape of the potential barrier, and the quasistatic (i.e. corresponding to conditions, when the temperature varies slightly) CVCs of the barrier.

2. Model Equation

Our calculations of parameters for varistor structures were based on a one-dimensional model of intergrain potential barrier (IPB), represented as two space charge regions (SCRs) in adjacent zinc oxide semiconductor crystallites connected oppositely to each other and separated by a thin (of a few nanometers) dielectric layer of the intergrain dielectric phase (IDP) [1, 2].

To determine the variation of the spatial distribution (the profile) of the donor concentration $N^+(x,t)$ in the boundary regions of zinc oxide crystallites (zinc oxide is an impurity semiconductor of the n-type) as a function of the degradation time t, we used the expression presented in work [21],

$$N^+(x,t_i+\Delta) = \\ = \frac{N^+(x,t_i)}{1-\frac{D^+}{L^2}\left[\frac{L_0}{D^+}\left(\sqrt{x^2-2D^+\Delta t}-x\right)-\Delta t\right]}, \qquad (1)$$

where $t_i (i = 0, 1, 2, \ldots, j)$ are the initial time moments for every following step Δt of the degradation time, D^+ is the diffusion coefficient for charged donors, x is the coordinate reckoned normally to the crystallite surface, e is the elementary charge, $L = \sqrt{\frac{\varepsilon_A \varepsilon_s kT}{e^2 N_0^+}}$ is the Debye screening length (for ZnO crystallites, $L \approx 10^{-6}$ cm), $L_0 \approx L\sqrt{Y_0}$ is the thickness of SCR in a semiconductor crystallite ($L_0 \sim 10^{-5}$ cm), and Y_0 is the dimensionless energy band bending in the semiconductor near its surface at the beginning of the degradation. Expression (1) was derived in the following manner:

– the Poisson equation was integrated taking into account that the influence of the free electron concentration $n(x,t)$ in near-surface SCRs, where $Y < 0$, can be neglected ($dY/dx = N^+(L_0 - x)/(N_0^+ L^2)$, where N_0^+ is the initial value of $N^+(x,t)$ at $t = t_0$);

– the result obtained was substituted into the continuity equation for migrating donor centers $N^+(x,t)$, taking into account that the distribution $N^+(x)$ changes smoothly enough in time t, if the time intervals of the degradation Δt are small, i.e. $\partial \int_0^x N^+(x',t)dx'/\partial t \approx x\partial N^+(x,t)/\partial t$; then, the analytical solution of the resulting continuity equation was obtained.

The potential distribution in the IPB – namely, the voltage drop across the reverse-biased, V_1, and direct-biased, V_2, SCRs in semiconductor layers and across the dielectric layer, V_3 – was determined from the conditions of potential and electric induction continuity at the interfaces "semiconductor layer of crystallite – insulating layer of the intergrain phase" [22]. The solution was obtained making the assumption that the current through the IPB is not so large that it could affect the distribution of charge carriers.

It should be noted that, at the degradation, it is necessary to consider a deviation of the IPB relief from the Schottky shape, for which $N^+(x,t) = \text{const}$, in the near-surface SCRs. This change takes place owing to a variation of the donor concentration distribution in the semiconductor according to Eq. (1). The coordinate dependence of the energy band bending Y can be found by numerically integrating the Poisson equation for SCR. This equation can be written down in the form of a boundary-value problem [21],

$$\frac{d^2Y}{d\tilde{x}^2} = \frac{e^2a^2}{\varepsilon_A\varepsilon_s kTL^2}\left[\widetilde{N}^+(\tilde{x}) - \tilde{n}(\tilde{x})\right]; \qquad (2)$$

$$Y(0,t) = Y_0; \qquad Y(L_0/L,t) = 0,$$

where $\tilde{x} = x/L$, $\tilde{n}(x) = n(x)/N_0^+$, $\widetilde{N}^+(x) = N^+(x)/N_0^+$, $n(x) = N^+(x)\exp(Y(x))$, and $2a$ is the linear size of a crystallite.

Using the finite difference method, we obtain a system of equations. The table of $Y(x_i)$-values is the solution of this system of equations,

$$Y_{i+1} - 2Y_i + Y_{i-1} - h^2 \frac{a^2}{L^2} \widetilde{N}_i^+ (1 - \exp(Y_i) = 0; \qquad (3)$$

$i = 1, 2, \ldots n-1,$

where $Y_n = 0$, $Y_i = Y(\tilde{x}_i)$, $\widetilde{N}_i^+ = \widetilde{N}^+(\tilde{x}_i)$, $h = L_0/(Ln)$, and $\tilde{x}_i = ih$. In Eqs. (2) and (3), the quantity $t = \text{const}$. Therefore, to make the record simpler, the dependence on this parameter was not included explicitly.

Quantitative calculations of CVCs for the IPB were carried out following the general scheme [22]. The latter was developed in the framework of the diode theory ideas concerning the penetration of charge carriers through potential barriers and making allowance for a complex of electrotransfer mechanisms, which are considered to be the most adequate to modern conceptions for oxide varistors [2, 20, 23]. In particular, these are the overbarrier (thermionic) emission with regard for the tunneling through a SCR, the field emission from the valence band of one crystallite into the conductance band of another one, and transitions with engaging the surface electron states at the contact.

The iteration algorithm for finding IPB CVCs is as follows:

1) the determination of surface band bendings $Y_0^{1,2}(x, t_0)|_{x=0}$ at both sides of the semiconductor layer at the moment t_0 ($t_0 = 0$) for reverse-biased (index 1) and direct-biased (index 2) SCRs by solving the system of equations following from the conditions of electric induction and potential continuity at the boundaries of the semiconductor layer taking Eq. (2) into account and for the given degradation voltage V_D in the Schottky approximation;

2) the application of Eq. (1) with the purpose to determine the profiles of the donor concentration distribution $N_{1,2}^+(x, t_i)$ in reverse- and direct-biased SCRs at the time moment $t_i = t_{i-1} + \Delta t$ ($i = 1, 2, \ldots$) and at the voltage V_D across the barrier;

3) the determination of equilibrium post-degradation ($V_D = 0$) surface band bendings $Y_0^{1,2}(x, t_0)|_{x=0}$ by solving the system of equations describing the continuity conditions of the electric induction and the potential with regard for Eq. (2); when determining the thickness L_0 in the second boundary condition (2), the equality $N_{1,2}^+ \approx (N_{1,2}^+(x, t_i))|_{x=0} + N_0^+)/2$ was adopted;

4) an analogous determination of post-degradation surface band bendings $Y^{1,2}(x, t_i)|_{x=0}$ in the case where the voltage $V \neq 0$ is applied to the IPB, and the corresponding voltage drops across reverse-biased, V_1, and direct-biased, V_2, SCRs, as well as across the dielectric layer, V_3;

5) the determination of profiles for the distributions of band bendings in the near-surface region (with the thickness L_0), $Y^{1,2}(x, t_i)$, by minimizing the objective function composed of the squares from Eqs. (3), in which the coordinate dependence $N_{1,2}(x, t_i)$ was taken into account;

6) the determination of the current density through the IPB following the routine described in work [22]; the values for dY^m/dx_m ($m = 1, 2$) were obtained by interpolating the numerical dependences of the coordinate in the band bending regions, $x_m(Y^m, t_i)$;

7) the repetition of items 4 to 6 in the whole necessary range of voltages in the calculation of CVCs;

8) the next iteration loop (items 2 to 7) till the given degradation time is achieved.

3. Results and Their Discussion

3.1. Variations of the charged donor distribution and the intergrain potential barrier relief

The donor distributions and the reliefs of potential barriers, which were calculated according to formulas (1)–(3) for various voltages V_D and degradation times t are depicted in Fig. 1.

As the quantities V_D and t grow, the donors are accumulated (the function $N^+(x)$ increases) in the boundary regions of semiconductor crystallites. In the SCR which is reverse-biased at the degradation, this effect is more pronounced; namely, the amount of accumulated donors is much higher, which corresponds to data obtained in work [13].

The limiting ($t \to \infty$) concentration distributions $N^+(x)$ were obtained as follows:

– the calculation of band bendings Y_0^1 and Y_0^2 by solving the system of equations, which consists of the continuity conditions for the electric induction and the potential at the interfaces between the semiconductor layer (the crystallite) and the dielectric layer of the intergrain phase, where $N_0^+ = n_{V0}$, $dY/dx = \sqrt{2}/LG(Y)$, and $G(Y) = \text{sign}(-Y)[\exp(-Y) + Y - 1 + \exp(Y) - Y - 1]^{1/2}$;

– the determination of the dependence $N^+(x) = N_0^+ \exp[-Y(x)]$, where $Y(x)$ satisfied the integral equation $\int_0^x \sqrt{2}/L dx = \int_{Y_0}^Y G(Y)^{-1} dY$.

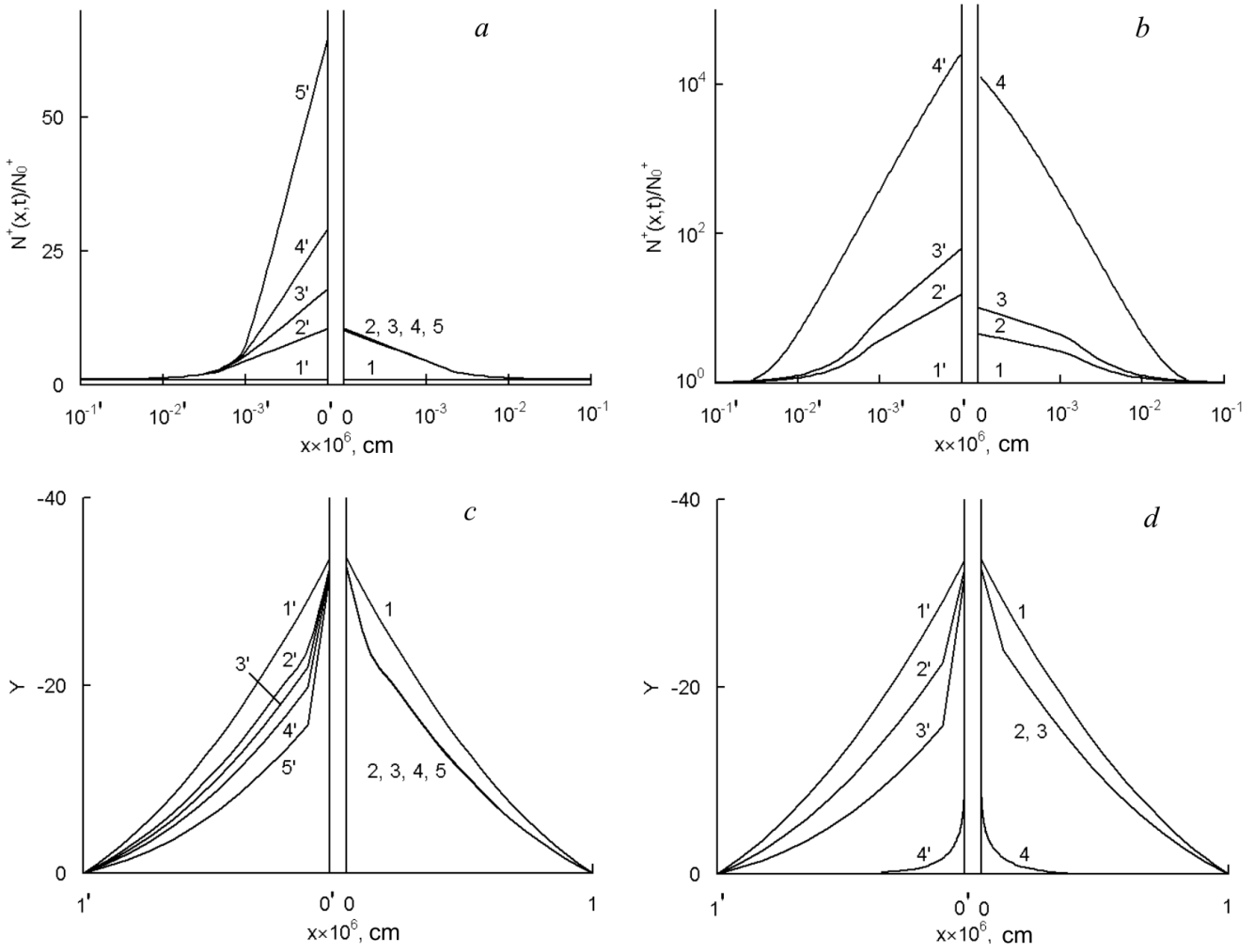

Fig. 1. Donor concentration profiles in the direction perpendicular to the surface of a semiconductor crystallite and the IPB relief in the near-surface SCRs of the semiconductor layer at a constant degradation time $\tilde{t} = tD^+/L^2 = 3400$ and various degradation voltages V_D (panels *a* and *c*): initial (*1, 1′*), 0 (*2, 2′*), 0.3 (*3, 3′*), 0.6 (*4, 4′*), and 1.2 V (*5, 5′*); and at the constant degradation voltage $V_D = 1.2$ V and various $\tilde{t}$ (panels *b* and *d*): 0 (*1, 1′*), 2200 (*2, 2′*), 3400 (*3, 3′*), and ∞ (4, 4′). Curves *2, 3, 4, 5* and *2′, 3′, 4′, 5′* correspond to direct- and reverse-biased, respectively, SCRs at the degradation current flow

The maximum concentrations of donors at their migration in the electric field are reached at the crystallite boundaries (Fig. 2). The growth of the degradation voltage V_D is not accompanied by considerable changes in the bulk donor concentration and the band bendings at the surface of semiconductor crystallites for the direct-biased SCR, with those quantities remaining practically unchanged. For the reverse-biased SCR, we obtained the dependence $N^+_{1,2}(0,t)$ growing with V_D and the dependence $Y_0(V_D)$ diminishing with increase in V_D at $t = \text{const}$, the both dependences tending to the corresponding constant values (Fig. 2, panels *a* and *c*). The dependences of $N^+_{1,2}(x,t)|_{x=0}$ on $\tilde{t}$, which correspond to the initial stage of degradation (at $V_D = \text{const}$), have a growing character (Fig. 2,*b*), which agrees with experimental data for varistor structures [3,13,24]. As a result, the intergrain barrier shape deforms as the degradation voltage and the time increase, and it becomes asymmetric. The thickness and the height of the potential barrier decrease.

The surface band bending for direct-biased SCR changes at the degradation less than that for the SCR biased by the degradation current in the opposite direction (Fig. 2,*d*). In addition, this SCR becomes less narrowed (curves 1 to 3 in Fig. 1,*d*). The IPB reliefs are exhibited under equilibrium conditions and after the degradation.

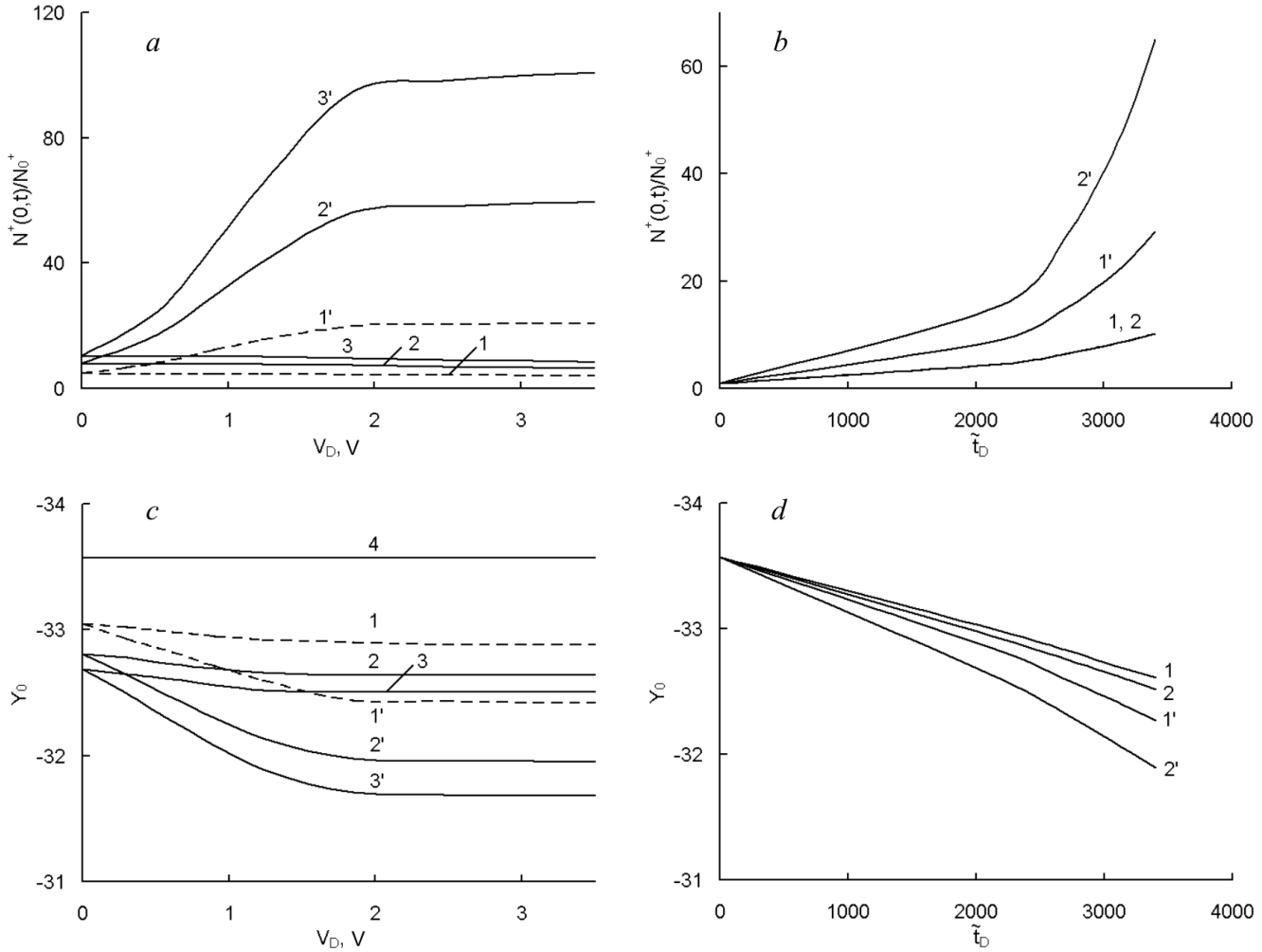

Fig. 2. Dependences of the donor concentration and the band bending at the semiconductor surface on the voltage V_D at various $\tilde{t}$ (panels *a* and *c*): 2200 (*1, 1′*), 3000 (*2, 2′*), 3400 (*3, 3′*), and the initial value (*4*); and on the degradation time $\tilde{t}$ at various V_D (panels *b* and *d*): 0.6 (*1, 1′*) and 1.2 V (*2, 2′*). Curves *1, 2, 3* and *1′*, *2′*, *3′* correspond to direct- and reverse-biased, respectively, SCRs at the degradation current flow

It should be noted that this tendency was also observed in work [3], when the degradation duration exceeded the variations of the indicated parameters (the IPB height and the bulk donor concentration) owing to the polarization and thermodesorption degradation mechanisms [7, 13].

The asymmetric character of the surface band bending at the boundaries of the intergrain phase manifests itself to a less extent (Figs. 1,*c* and *d*). This occurs due to the action that the field of charges accumulated at the surface electron states of one crystallite exerts in the region of another crystallite through the nano-sized interlayer.

As the duration and the voltage of the degradation increase, the deformation of IPB grows and results in the almost total disappearance of the latter (curves *4* and *4′* in Fig. 1,*d*).

3.2. Distortion of voltage-current characteristics of the intergrain potential barrier

The results of calculations of CVCs for a certain IPB are depicted in Fig. 3. The CVC branches in the first quadrant (straight lines) correspond to the positive voltage V and the current density j, which coincide by direction with the voltage, V_D, and the current, j_D, of the degradation. The CVC branches in the third quadrant (the reverse ones) correspond to the negative voltage V and the current density j, the direction of which is op-

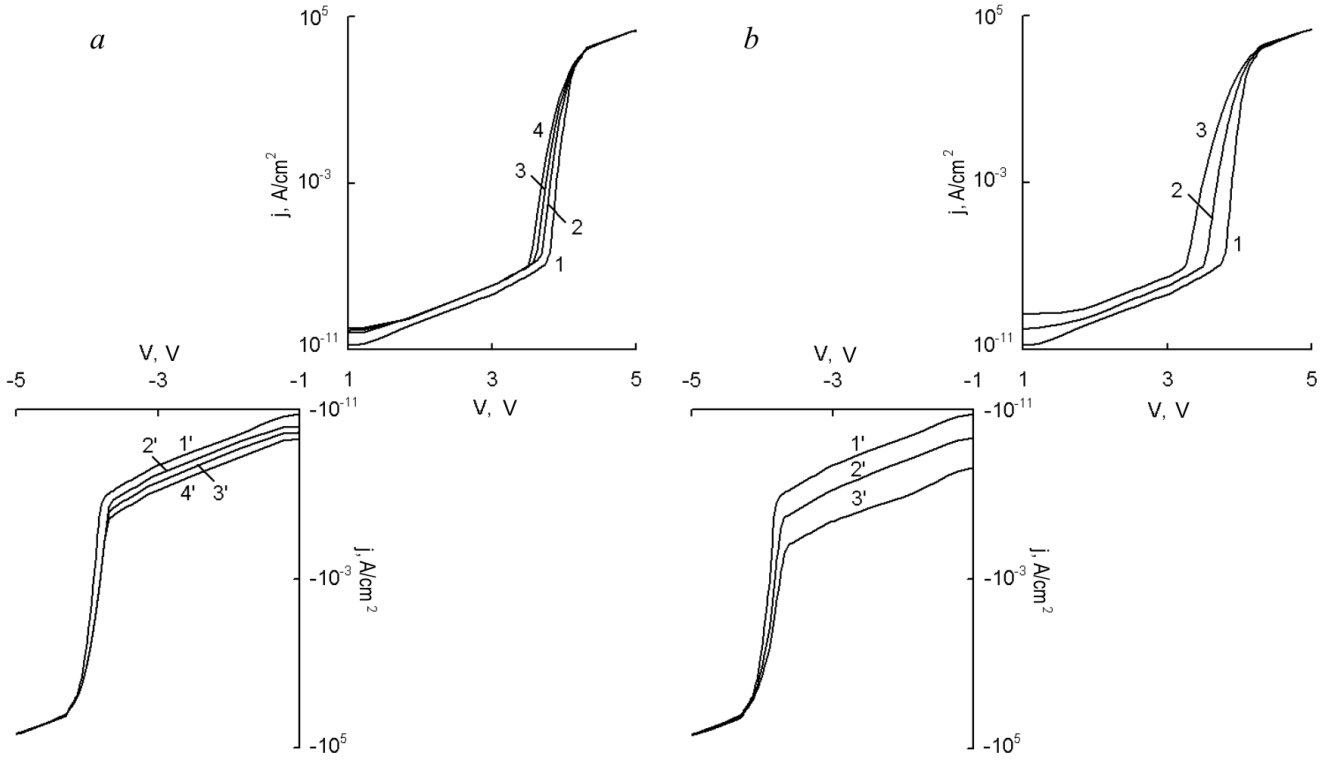

Fig. 3. CVCs of a separate IPB at the constant degradation time $\tilde{t} = tD^+/L^2 = 2200$ and various degradation voltages V_D (panel *a*): initial (*1*, *1′*), 0 (*2*, *2′*), 0.6 (*3*, *3′*), and 1.2 V (*4*, *4′*); and at the constant degradation voltage $V_D = 1.2$ V and various degradation times $\tilde{t}$: 0 (*1*, *1′*), 2200 (*2*, *2′*), and 3400 (*3*, *3′*)

posite to that of V_D and j_D. According to the data presented in Fig. 3, the electromigration processes lead to a shift of both CVC branches toward higher currents at a fixed voltage, $V = \text{const}$, or toward lower voltages at $j = \text{const}$, and to their asymmetry, which corresponds to experimental data [24].

A physical interpretation of those results can be given on the basis of conceptions concerning the formation of CVC for the IPB [1, 2] and the data on the features of its distortion presented above. The current density through the potential barrier at the contact is known to be governed by the magnitude of band bending in the direct-biased SCR [22, 25]. According to those ideas, a reduction of the IPB thickness and height owing to the accumulation of donors that migrate in the electric field gives rise, first of all, to an increase of such current components through the barrier as the thermionic emission and the electrotransfer with the participation of surface electron states. In particular, a larger reduction of the height and the thickness of reverse-biased SCR at the degradation brings about a larger leakage current in the weakly nonlinear section of the reverse CVC branch for the varistor structure.

On the other hand, a reduction of the IPB thickness results in that the current increases at the tunnel electrotransfer from the valence band of one crystallite into the conduction band of the other, i.e. the highly nonlinear section of the CVC shifts toward lower voltages (see Fig. 3). At the field emission, the charge carrier overcomes a distance equal to a sum of the thicknesses of the interlayer and the reverse-biased SCR in the other crystallite. Since the thickness of SCR, which is reverse-biased at the degradation, becomes narrower, the shift of the direct CVC branch toward low voltages is larger.

3.3. Degradation-induced changes in varistor parameters

The electromigration degradation brings about a CVC distortion for the intergrain potential barrier, which, in turn, results in a worsening of functional parameters of metal oxide varistor structures. In particular, the growth of the degradation voltage and duration is responsible for the following phenomena:

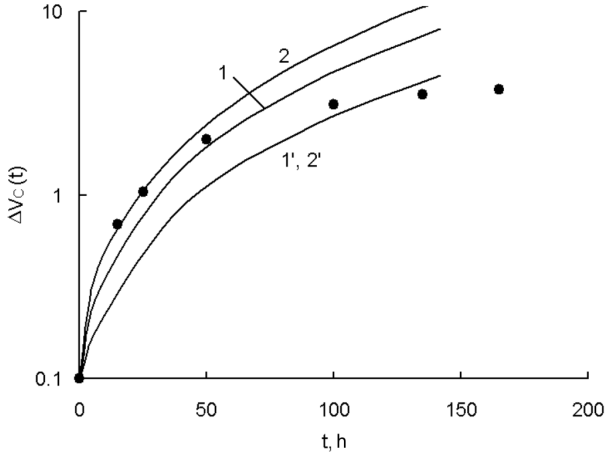

Fig. 4. Dependences of the classification voltage deflection ΔV_C on the duration of a constant degradation electric current j_D. Curves represent the results of theoretical calculations for a single IPB at various degradation voltages $V_D = 0.3$ (*1, 1′*) and 1.2 V (*2, 2′*). Curves *1* and *2* correspond to measurements in the degradation current direction, and curves *1′* and *2′* to the measurements in the opposite direction. Points denote the experimental results for a varistor structure [24] obtained at the j_D-polarity, for which the deflection ΔV_C is maximal

– a reduction of the classification voltage V_C (it is the voltage that corresponds to the start of the varistor section in the CVC; $V_C = V$ at $j_C = 10^{-4}$ A/cm^2), which is determined by the deflection parameter $\Delta V_C = [V_C(t_D) - V_C(0)]/V_C(0) \times 100\%$ at $j \approx 0.1 j_C$ [24];
– a reduction of the CVC nonlinearity factor β in the varistor section, $\beta = \ln(j_2/j_1)/\ln(V_2/V_1)$, where it is adopted that $j_2 = j_C$, $j_1 = 0.1 j_C$, $V_2 = V_C$, and $V_1 = V$ at $j = j_1$;
– an increase of the leakage current density $j0$ in the slightly nonlinear CVC section, which corresponds to the voltage $V = 0.8 V_C$ [24].

The dependences of CVC parameters on the degradation voltage and time are given in Figs. 4 and 5. These figures also present the results of experimental researches concerning the influence of the long-term passage of a constant electric current with a density of about 10^{-5} A/cm^2 [1, 2, 24], which corresponds to a mode of standard industrial tests, on the stability of varistor zinc oxide structures. The values of voltage V_D applied at the degradation across a separate IPB, provided that the current density j_D was equal to that used under test conditions (at a temperature of 358 K), corresponded to the interval from 0.5 to 1.5 V. The transition from the dimensionless degradation time, $\tilde{t}$, used in theoretical calculations to the real one, t, was carried out by selecting the diffusion coefficient for donor ions, D^+, so that the

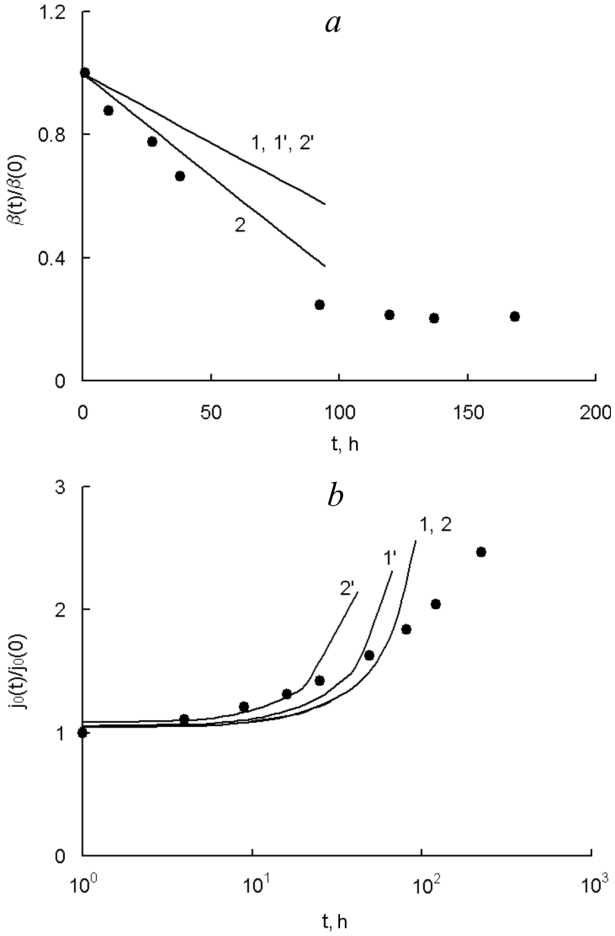

Fig. 5. Dependences of the CVC nonlinearity factor β (a) and the leakage current (b) on the time of a constant degradation electric current flow, t. Curves represent the results of theoretical calculations for a single IPB at various degradation voltages $V_D = 0.3$ (*1, 1′*) and 1.2 V (*2, 2′*). Curves 1 and 2 correspond to measurements in the degradation current direction, and curves *1′* and *2′* to the measurements in the opposite direction. Points denote experimental results for a varistor structure [18, 24] obtained at the j_D-polarity, for which the deflection ΔV_C is maximal

best coincidence with the initial sections of the considered dependences should be provided. This was achieved by moving the curves along the logarithmic time scale. The obtained estimates for D^+ ranged from 1×10^{-15} to 5×10^{-15} cm^2/s for data reported in works [18, 24], which agrees with the data known for polycrystalline zinc oxide [26].

By analyzing the time dependence of a deflection of the classification voltage, $\Delta V_C(t)$, we may state a satisfactory correspondence between experimental data and the results provided by the considered model for short time intervals of the degradation electric current flow.

However, with the growth of t, the experimental dependence testifies to a slower increase of the parameter under consideration. The most probable reason for this discrepancy is the inhomogeneity of the ceramic structure and the percolation character of its electrical conductivity [27]. In the course of degradation, the resistance of critical barriers (in terms of work [28]) decreases owing to their distortion. This can lead to the equalizing of resistances in the circuits of the critical sublattice.

Hence, in the course of degradation, owing to a reduction of critical IPB resistances, a redistribution of the voltage can take place in the varistor structure. As a result, the period of the critical sublattice can decrease, and the voltage applied across such a separate IPB also decreases, which manifests itself in a reduction of the deflection, ΔV_C, sensitivity to the voltage applied to the structure.

It should be noted that, by analogous reasons, we observed a slower increase of other experimental CVC parameters (β and j_0) as well.

To summarize, it should be noted that the procedure of determination of the electrodiffusion coefficient of ionized donors D^+, which was considered here, allows conclusions on the stability and the service lifetime of a varistor structure to be drawn.

4. Conclusions

An electromigration model describing a variation of the nonlinear electric properties of non-uniform structures with intergrain potential barriers during the long-term passage of an electric current has been developed. The model allows the irreversible degradation of those structures to be interpreted properly. The electric current through the intergrain potential barrier in a structure composed of semiconductor crystallites separated by a thin (of about 20 Å) dielectric layer gives rise to a growth of the donor concentration near the crystallite surface owing to the donor motion in the electric field, as well as to a distortion of the barrier and the current-voltage characteristics of the structure. The SCR, which is reverse-biased at the degradation current flow, is more prone to a distortion (the accumulation of near-surface donor concentration, a reduction of the height and the thickness of the intergrain barrier). In the course of degradation, the varistor section in the direct (with respect to the degradation current) CVC branch turns out more shifted toward lower voltages, and the leakage current grows more rapidly in the weakly nonlinear section of the reverse CVC branch. A correlation between the tendencies for main varistor parameters to change (a reduction of the classification voltage, a reduction of the nonlinearity factor, and an increase of the leakage current) has been established by analyzing the developed model and the known experimental data. We have demonstrated that the data obtained can be applied to the estimation of the diffusion coefficient of charged donors. This parameter can be used for the estimation of the stability and the service lifetime of products on the basis of varistor zinc oxide structures with tunnel current-voltage characteristics.

1. Kh.S. Valeev and V.B Kvaskov, *Nonlinear Metal-Oxide Semiconductors* (Energoizdat, Moscow, 1983) (in Russian).
2. T.K. Gupta, J. Am. Ceram. Soc. **73**, 1817 (1990).
3. A.S. Tonkoshkur, A.Yu. Lyashkov, I.V. Gomilko, and A.V. Ivanchenko, Neorg. Mater. **36**, 892 (2000).
4. Dogxiang Zhou, Gongchun Zhang, and Shuping Gong, Mater. Sci. Eng. B **99**, 412 (2003).
5. H.S. Domingos, J.M. Carlsson, P.D. Bristowe, and B. Hellsing, Interface Sci. **12**, 227 (2004).
6. B.H. Lee and S.M. Kang, Curr. Appl. Phys. **6**, 844 (2006).
7. Jun Liu, Jinliang He, Jun Hu, Wangcheng Long, and Rong Zeng, J. Am. Ceram. Soc. **93**, 2473 (2010).
8. A. Iga, Jpn. J. Appl. Phys. **19**, 201 (1980).
9. B.K. Avdeenko, A.S. Tonkoshkur, I.M. Chernenko, A.I. Ivon, and A.I. Shchelokov, Elektron. Tekhn. Ser. 5. Radiodet. Radiokomp. **41**, 17 (1980).
10. V.O. Makarov, A.S. Tonkoshkur, and I.M. Chernenko, Elektron. Tekhn. Ser. 5. Radiodet. Radiokomp. **70**, 18 (1988).
11. P. Kjstic, O. Milosevic, D. Uskovic, and M.M. Ristic, Physica B+C **150**, 175 (1990).
12. W. Moldenhauer, K.H. Bather, W. Bruckner *et al.*, Phys. Status Solidi A **67**, 533 (1981).
13. Y.H. Chiang and W.D. Kingery, J. Appl. Phys. **53**, 1765 (1982).
14. A.V. Ivanchenko and A.S.Tonkoshkur, in *Photoelectronics,* (Astroprint, Odessa, 2003), Vol. 12, p. 18 (in Russian).
15. A.V. Ivanchenko, A.S. Tonkoshkur and V.O. Makarov, J. Eur. Ceram. Soc. **24**, 3709 (2004).
16. K. Eda, A. Iga, and M. Matsuoka, J. Appl. Phys. **51**, 2678 (1980).
17. T.K. Gupta and W.D. Carlson, J. Mater. Sci. **20**, 3347 (1985).

18. K. Sato and Y. Takada, J. Appl. Phys. **53**, 8819 (1982).

19. Sh. M. Gansali and A.M. Gashimov, Probl. Energet. No. 2, 67 (2005).

20. V.B. Kvaskov, *Semiconductor Devices with Bipolar Conductivity* (Energoatomizdat, Moscow, 1988) (in Russian).

21. A.V. Ivanchenko and A.S. Tonkoshkur, Multidisc. Model. Mater. Struct. **3**, 477 (2007).

22. A.S. Tonkoshkur, Elektron. Tekhn. Ser. 5. Radiodet. Radiokomp. **83**, 15 (1991).

23. R. Einzinger, in *Polycrystalline Semiconductors: Physical Properties and Applications*, edited by G. Harbeke (Springer, New York, 1985), p. 228.

24. A.S. Tonkoshkur, I.M. Chernenko, and V.L. Subbota, Neorg. Mater. **31**, 791 (1995).

25. V.I. Strikha, *Contact Phenomena in Semiconductors* (Vyshcha Shkola, Kyiv, 1982) (in Russian).

26. I.P. Kuzmina and V.A. Nikitenko, *Zinc Oxide. Synthesis and Optical Properties* (Nauka, Moscow, 1984) (in Russian).

27. A.S. Tonkoshkur, Fiz. Tverd. Tela **32**, 2260 (1990).

28. B.I. Shklovskii and A.L. Efros, *Electronic Properties of Doped Semiconductors* (Springer, Berlin, 1984).

Received 17.02.11.
Translated from Ukrainian by O.I. Voitenko

ЕЛЕКТРОМІГРАЦІЙНА МОДЕЛЬ ДЕГРАДАЦІЇ МЕТАЛОКСИДНИХ ВАРИСТОРНИХ СТРУКТУР

О.В. Іванченко, О.С. Тонкошкур

Р е з ю м е

Наведено результати моделювання впливу міграції іонів у напівпровідникових кристалітах оксиду цинку при тривалому протіканні робочого електричного струму на вольт-амперні характеристики варисторних структур і визначення умов та параметрів, придатних для контролю процесу їхньої незворотної деградації.

Встановлено, що більш схильна до змін (накопичення приповерхневої концентрації донорів, зменшення висоти й товщини) складова міжкристалітного потенціального бар'єра, яка утворюється областю просторового заряду кристаліта, є зворотно зміщеною під час протікання деградаційного струму. У процесі деградації варисторна ділянка прямої (стосовно струму деградації) гілки вольт-амперної характеристики (ВАХ) більше зміщується в область менших напруг, а струм витоку більше зростає для слабонелінійної ділянки зворотної гілки ВАХ.

Показано відповідність тенденцій зміни основних варисторних параметрів (зниження класифікаційної напруги, зменшення коефіцієнта нелінійності та збільшення струму витоку), котрі одержані з аналізу розвинутої моделі, відомим експериментальним даним і можливість оцінки коефіцієнта дифузії заряджених донорів та використання цього параметра у контролі працездатності виробів на основі варисторних оксидно-цинкових структур з тунельною вольт-амперною характеристикою.